Optimizing stilbene recovery from cell cultures media: A comprehensive study of the adsorption process

Ruxandra Toma, Julien Lemaire, Amandine Flourat, Blandine Marant, Mathilde Duval, Florent Allais, Morad Chadni

Optimizing stilbene recovery from cell cultures media: A comprehensive study of the adsorption process

Ruxandra Toma[1], Julien Lemaire[2], Amandine L. Flourat[1], Blandine Marant[3], Mathilde Duval[4], Florent Allais[1], Morad Chadni[*,1]

DOI : https://doi.org/10.1016/j.seppur.2024.128983

[1] URD Agro-Biotechnologie Industrielles, CEBB, AgroParisTech, 51110 Pomacle, France
[2] Université Paris-Saclay, CentraleSupélec, Laboratoire de Génie des Procédés et Matériaux, Centre Européen de Biotechnologie et de Bioéconomie (CEBB), 3 rue des Rouges Terres, 51110 Pomacle, France
[3] Université de Reims Champagne Ardenne, INRAE, RIBP USC 1488, 51100 Reims, France
[4] Novéal, 16 Rue Maurice Berteaux, 95500 Le Thillay, France

* Correspondence: morad.chadni@agroparistech.fr

Abstract

Stilbenes are of significant interest due to their potential health benefits and applications in pharmaceuticals and nutraceuticals. Traditional extraction methods often involve organic solvents, which pose environmental and safety concerns.This study investigates the extraction of stilbenes (E-resveratrol, labruscol, leachianol, ε-viniferin, and δ-viniferin) from grapevine (*Vitis vinifera and Vitis labrusca*) cell cultures using adsorption technology. Five food-grade resins (XAD-7, XAD-16, XAD-4, XAD-1180, and FPX-66) were tested for stilbene adsorption. XAD-7 was chosen as the optimum adsorbent, displaying the highest adsorbed quantity (86.94 ± 4.90 $mg_{stilbenes}/g_{dry\ resin}$) and desorbed quantity (74.28 ± 0.38 $mg_{stilbenes}/g_{dry\ resin}$). Adsorption kinetics using XAD-7 followed a pseudo-second-order model, with intraparticle diffusion limiting approximately 10% of total adsorption. Desorption occurs more rapidly than adsorption, achieving equilibrium in about 60 min. Isotherm curves fitted well to a multicomponent Langmuir model, indicating a maximum adsorption capacity of 0.280 to 0.360 $mmol_{stilbenes}/g_{dry\ resin}$, close to the experimental value of 0.271 $mmol_{stilbenes}/g_{dry\ resin}$. Stilbene affinity for XAD-7 decreased in the following order: ε-viniferin > (labruscol, E-resveratrol, leachianol) > δ-viniferin. The optimal desorbed quantity of 59.74 ± 0.14 $mg_{stilbenes}/g_{dry\ resin}$ was achieved with a 70% ethanol solution and a 160:1 desorption solution-to-adsorbent ratio (v/w). XAD-7 resin coupled with an optimized washing step increased stilbene purity by 4.6 times (from 5.41 ± 0.05% to 23.19 ± 0.31% w/w). XAD-7 can be reused for multiple cycles with consistent adsorption capacity and desorption yield, maintaining the same stilbenes purity after 5 cycles.

This study underscores the viability of polymeric resin adsorption as an eco-friendly and efficient method for stilbene extraction from grapevine cell cultures, paving the way for sustainable production processes in the nutraceutical and pharmaceutical industries.

Key words: Stilbenes, resins, adsorption, purification, resveratrol, grapevine cell cultures, phenolic compounds, antioxidants

1. Introduction

Polyphenolic compounds represent one of the largest categories of plant secondary metabolites, which are segmented in different classes based on their structure, the most important ones being stilbenes, flavonoids and phenolic acids. Naturally occurring stilbenes are biosynthesized as a defensive response to abiotic or biotic stresses, such as high temperatures, excessive ultraviolet radiations, bacterial or fungal infections [1]. Owing to the presence of phenolic moieties, stilbenes are distinguished by pronounced antioxidant effects and concurrently exhibit a spectrum of properties, including antimicrobial, antifungal, anti-inflammatory, anti-aging, anti-diabetic, anti-degenerative, antitumor, and neuroprotective activities [2]. Therefore, they exhibit great potential in preventive and/or therapeutic applications, and thus generate an interest for new drug research and development.

1,038 different stilbenes have been identified and isolated until now [3]. Stilbenes are predominantly present mainly in 11 plant families (*Vitaceae, Dipterocarpaceae, Gnetaceae, Stemonaceae, Cyperaceae, Asparagaceae, Moraceae, Orchidaceae, Euphorbiaceae, Leguminosae*) [3]. Stilbenes are commonly extracted from plant systems, which represent the primary sources of these secondary metabolites. They have been reported to be extracted from many different plants or plant by-products, such as spruce bark [4], Japanese knotweed [5], mulberry twigs, mango pulp, Smilax China root, Carex plant species [6] and viticultural or wine manufacturing by-products (grape canes, young lateral shoots, grape marc and leaves) [7]. Resveratrol and some stilbene derivatives can also be synthesized chemically or through biocatalysis [8–12].

Biotechnological processes offer an efficient and sustainable alternative for stilbene production through the utilization of plant cell cultures, addressing the limitations associated with extraction from plant materials or chemical synthesis. Production from plant cell cultures has been widely investigated for stilbenes production, by using specific elicitors (e.g., ultraviolet irradiation, methyl jasmonate or cyclodextrin) to increase the product yield [13]. In 2022, Aneklaphakij et al., summarized research on resveratrol biosynthesis from plant cell cultures, including *Arachis hypogaea, Artocarpus lacucha, Morus alba,* and various *Vitis* species [14].

Obtention of high purity stilbene derivatives was reported by using silica gel column chromatography for fractionation of plant extracts into several stilbene fractions, followed by their purification using semipreparative HPLC [15] or by centrifugal partition chromatography [12,16]. Despite the very high purity of the compounds obtained by these chromatographic techniques, their feasibility for industrial applications is very limited as they are laborious, expensive, and create large amounts of solvent wastes [17]. Adsorption by macroporous resins has been widely studied in the past years for the separation and purification of polyphenols. Compared to other alternative separation methods, the adsorption-desorption process involves easier design, operation and maintenance, less installation costs, minimal environmental harm, and it also presents great efficiencies [18]. Moreover, the use of food-grade resins

represents an advantage for the recovery of molecules which are intended to be used in specific fields. Table 1 summarizes several research papers which used macroporous adsorbent resins, such as the Amberlite XAD series, RENSA or ADS resins, for the adsorption of stilbenes or other polyphenols.

Table 1. Research on the adsorption of stilbenes and other polyphenolic compounds with macroporous Resins

Compound	Source	Macroporous resin	Adsorption quantity or yield	Desorption yield	Reference
Resveratrol	*Corynebacterium glutamicum*	Amberlite XAD-7HP	12.5 $mg_{resveratrol}/g_{wet\ resin}$	-	[19]
Resveratrol	Model solution	Amberlite XAD-7HP Amberlite XAD-16 RENSA PX RENSA PY	11 $mg_{resveratrol}/g_{wet\ resin}$ 18 $mg_{resveratrol}/g_{wet\ resin}$ 80 $mg_{resveratrol}/g_{wet\ resin}$ 58 $mg_{resveratrol}/g_{wet\ resin}$	-	[20]
Resveratrol	Extract of peanut sprout	ADS-21 ADS-7 ADS-17 ADS-5 AB-8 S-8 NKA-9 NKA-II HPD-600 X-5 D101	~ 26.7 $mg_{resveratrol}/g_{resin}$ ~ 24.6 $mg_{resveratrol}/g_{resin}$ ~16.8 $mg_{resveratrol}/g_{resin}$ ~ 25.3 $mg_{resveratrol}/g_{resin}$ ~ 23.9 $mg_{resveratrol}/g_{resin}$ ~ 25.3 $mg_{resveratrol}/g_{resin}$ ~ 21.5 $mg_{resveratrol}/g_{resin}$ ~ 18.9 $mg_{resveratrol}/g_{resin}$ ~ 13 $mg_{resveratrol}/g_{resin}$ ~ 18 $mg_{resveratrol}/g_{resin}$ ~ 15.8 $mg_{resveratrol}/g_{resin}$	~ 47.6 % ~ 54.3 % ~ 60.9 % ~ 88.43 % ~ 84.1 % ~ 42.1 % ~ 73.8 % ~ 70.7 % ~ 63.8 % ~ 77.6 % ~ 75.9 %	[21]
Chlorogenic acid	Aqueous permeate obtained from purification of sunflower protein	Amberlite XAD-4 Amberlite XAD-7 Amberlite XAD-16 Amberlite XAD-1180 HP20	14.07 $mg/g_{dry\ resin}$ 12.03 $mg/g_{dry\ resin}$ 15.32 $mg/g_{dry\ resin}$ 12.62 $mg/g_{dry\ resin}$ 11.21 $mg/g_{dry\ resin}$	90% for XAD7 and XAD16	[22]
Total phenolic compounds	*Vitis vinifera L.* pomace extract	LXA-10	4.86 mg/g	-	[23]
Total phenolic compounds	Coffee grounds extract	Amberlite XAD-7 Amberlite XAD-16 Amberlite XAD-1180 Amberlite XAD-4 Amberlite XAD-2	~ 52% ~ 78% ~ 76% ~ 48% ~ 61%	~ 100% ~ 88% ~ 72% ~ 79% ~ 82%	[24]
Total flavonoids	Extracts from *Nymphaea lotus* L. stamen	Amberlite XAD-2 Amberlite XAD-4 Amberlite XAD-16 Amberlite XAD-7 DAX8	~ 87.1% ~ 74.5% ~ 82.2% ~ 93.3% 94.37%	~ 76.6% ~ 75.8% ~ 78.1% ~ 91.5% ~ 92%	[25]

The objective of this work is the purification of resveratrol and four resveratrol dimers from the supernatant of *Vitis vinifera* cell cultures. Firstly, several macroporous adsorbent resins were tested for a preliminary screening step to determine the optimum polymeric adsorbent. The second step consisted of studying the kinetics of adsorption by following the evolution of the adsorbed and desorbed quantity of stilbenes. Two kinetics-based models (pseudo-first and pseudo-second order) and one diffusion-based model (intraparticle diffusion) were used to interpret the process. Thirdly, adsorption isotherms were studied using a multicomponent Langmuir model taking into account the competition between the

stilbenes. Finally, experiments were conducted to optimize various process parameters, such as the ratio and ethanol content of the desorption solution, but also influence of the water quantity, pH, and washing time on the final purity of stilbenes.

2. Material and methods

2.1. Chemicals

Labruscol (Lab) (Purity > 98 %), leachianol (Lea) (Purity > 98%), and δ-viniferin (δ-Vin) (Purity > 98 %), standards were synthesized in house following the procedure described by [12]; *E*-resveratrol (*E*-Res) (Purity > 99 %), and ε-viniferin (ε-Vin) (Purity > 99 %), standards were purchased from Interchim and PhytoLab, respectively. All inhouse synthesized stilbenes were assessed by NMR then HPLC to ensure solely the peak of desired compound is present. It is to notice that, in case of labruscol, two peaks are present and relate to the two diastereoisomers. The chemical structure of the studied stilbenes is presented in Figure 1. The study focused on these five stilbenes because they are the only ones produced by the grapevine cell strains under the specific culture conditions. Methanol and ethanol (≥ 99.5% purity) were purchased from Fisher Scientific™. Anhydrous acetonitrile and spectroscopic grade methanol were purchased from VWR Chemicals. Milli-Q water was produced by a Milli-Q® Integral Water Purification system from Millipore.

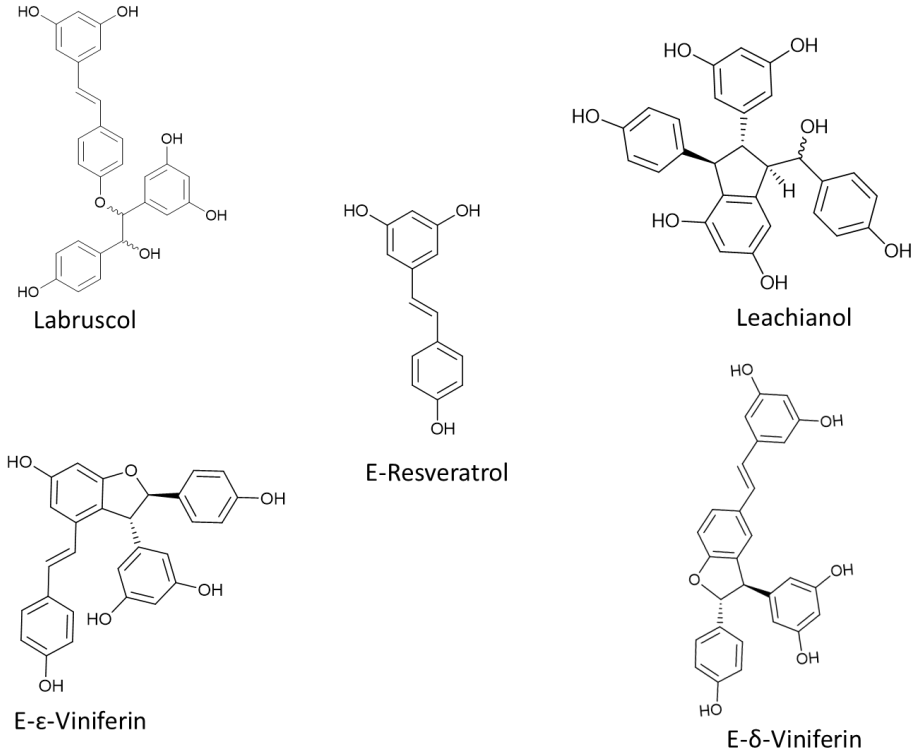

Figure 1. Chemical structures of E-resveratrol, E-ε-viniferin, E-δ-viniferin, leachianol and labruscol.

2.2. Plant cell cultures extracellular media

Different batches of grapevine cell cultures (*Vitis labrusca* and *Vitis vinifera*) elicited with 50 mM of Methyl-β-cyclodextrins and 0.5 mM of methyl jasmonate were performed using 2 L bioreactor

(Minifors) and 10 L bioreactor (Sartorius). Cells and medium obtained from the different batches were separated under reduced pressure using a nylon filter (20 µm), to conserve the medium containing the stilbenes at -20 °C.

2.3. Resin preparation

Five polymeric macroporous resins (XAD-7, XAD-16, XAD-4, XAD-1180 and FPX-66) from the AmberLite™ series were initially screened for their adsorption capacities. The resins properties are presented in Table S1 in supplementary material file. All resins required a pretreatment step before usage to remove residual monomeric units remained from the manufacturing process and undesired salts. The resins were rinsed twice with Milli-Q water, followed by washing for 15 hours with Milli-Q water. Afterwards, the resins were filtered (Buchner filtration system, nylon filter of 20 µm) and washed with methanol for 2 hours. Finally, methanol was removed by filtration and the resins were rinsed three times and washed for 4 hours with Milli-Q water. All steps were performed in an ES-20/60 Orbital Shaker-Incubator (Biosan. Lettonie) at 25 ºC and 130 rpm at a ratio of 5 mL to 1 g of resin. At the end, the resins were dried using a Buchner filtration system and the moisture content was determined using a MB35 moisture analyzer (Ohaus/ Switzerland).

2.4. Resins screening

In order to find the optimum macroporous resin for stilbenes purification, an initial step of resins screening was performed by carrying out adsorption and desorption experiments. The adsorption tests were conducted as follows: 0.5 g of dry resin and 20 mL of culture medium (40:1 ratio) were added in 125 mL shake flasks covered with parafilm and aluminum foil and agitated for 15 hours (140 rpm, 25 ºC), until equilibrium was reached. Afterwards, the culture medium was separated by filtration and analyzed by HPLC. The resins were washed with 30 mL of Milli-Q water (60:1 ratio) and introduced with 100 mL of 70% EtOH desorption solution (200:1 ratio) into 125 mL shake flasks covered with parafilm and aluminum foil. The flasks were shaken for 15 hours (180 rpm, 25 ºC). Finally, the desorption solutions were separated from the resins beads by filtration and analyzed by HPLC. The adsorption/desorption performance of different resins was assessed by calculating the quantity of stilbene adsorbed then desorbed, and derived parameters according to following equations:

$$q_{eq,i} = \frac{(C_{0,i} - C_{eq,i}) \times V_s}{W} \quad \text{Eq (1)}$$

$$SA_i = \frac{(C_{0,i} - C_{eq,i}) \times V_s}{W \times SS} \quad \text{Eq (2)}$$

$$q_{d,i} = \frac{C_{d,i} \times V_d}{W} \quad \text{Eq (3)}$$

$$A_i\ (\%) = \frac{C_{0,i} - C_{eq,i}}{C_{0,i}} \times 100 \qquad \text{Eq (4)}$$

$$D_i\ (\%) = \frac{C_{d,i} \times V_d}{(C_{0,i} - C_{eq,i}) \times V_s} \times 100 \qquad \text{Eq (5)}$$

Where $\boldsymbol{q_{eq,i}}$ is the adsorbed quantity of stilbene i at equilibrium (mg/g of dry resin); $\boldsymbol{SA_i}$: surface adsorbed quantity of stilbene i at equilibrium (mg/m^2); $\boldsymbol{q_{d,i}}$: desorbed quantity of stilbene i at equilibrium (mg/g of dry resin); $\boldsymbol{A_i}$ and $\boldsymbol{D_i}$ are adsorption and desorption yields (%), respectively; $\boldsymbol{C_{0,i}}$, $\boldsymbol{C_{eq,i}}$ and $\boldsymbol{C_{d,i}}$ are the concentrations of stilbene i initially, after adsorption then after desorption at equilibrium (mg/mL) respectively; $\boldsymbol{V_s}$ and $\boldsymbol{V_d}$ are the volumes of culture medium and desorption solution (mL) respectively; $\boldsymbol{W}$ is the resin dry weight (g); $\boldsymbol{SS}$ is the resin specific surface (m^2/g); i refers to *E*-resveratrol, leachianol, labruscol, δ-viniferin, or ε-viniferin.

2.5. Adsorption kinetics

The adsorption kinetics tests were performed as follows: 0.75 g of dry resin and 30 mL of grapevine cell culture medium (40:1 ratio) were added in 125 mL shake flasks covered with parafilm and aluminum foil and shaken for 24 hours (140 rpm, 25 ºC). The adsorbed quantity of each stilbene was calculated at 5, 10, 15, 20, 25, 30, 35, 40, 50, 60, 90, 120, 180, 240, 300 and 360 minutes by quantifying their remaining amount in the liquid phase by HPLC. Afterwards, the resins were collected by filtration and desorbed with 150 mL of 70% ethanol solution under agitation (200 rpm, 25 ºC). The desorbed quantity of each stilbene was calculated for six hours at the same time points mentioned above, by quantifying their amount recovered in the desorption solution by HPLC. Both non-linear and linear forms of the Pseudo-first order (PFO) and Pseudo-second order (PSO) models and the linear form of the intra-particle diffusion model were used to fit the experimental data. All the corresponding equations are shown in Table S2 in supplementary material.

2.6. Adsorption isotherms

The Langmuir model is a commonly used mathematical model to describe experimental adsorption isotherms [13,21], and it was also chosen to be applied in the current work. The underlying assumptions of this mechanistic equilibrium model are that molecules adsorption leads exclusively to the formation of a monolayer, on active sites considered homogeneous, identical and with equal accessibility. Moreover, it assumes no interaction between compounds adsorbed on nearby sites. When studying the behavior of systems with multiple components which have different affinities for the absorbent, researchers have developed Langmuir models without competition (different molecules are adsorbed on specific site) or with competition when it is more relevant to consider that all molecules are adsorbed on the same type of site [26]. This competitive model was chosen herein because it was considered that the different stilbenes are most probably adsorbed on the same type of site, due to their similar chemical

structure [13]. The combination of Langmuir and mass balance equations for the five stilbene molecules leads to Equations Eq (**6**) - **Erreur ! Source du renvoi introuvable.** after basic simplification.

$$C_{eq,Res} = \frac{C_{0,Res} \cdot \left(\frac{V_S}{W}\right)}{\left(\frac{V_S}{W}\right) + \frac{K_{eq,Res} \cdot qmax}{1+K_{eq,Res} \cdot C_{eq,Res} + K_{eq,Lae} \cdot C_{eq,Lae} + K_{eq,Lab} \cdot C_{eq,Lab} + K_{eq,\delta-\mathrm{Vin}} \cdot C_{eq,\delta-\mathrm{Vin}} + K_{eq,\varepsilon-\mathrm{Vin}} \cdot C_{eq,\varepsilon-\mathrm{Vin}}}} \quad \text{Eq (6)}$$

$$C_{eq,Lab} = \frac{C_{0,Lab} \cdot \left(\frac{V_S}{W}\right)}{\left(\frac{V_S}{W}\right) + \frac{K_{eq,Lab} \cdot qmax}{1+K_{eq,Res} \cdot C_{eq,Res} + K_{eq,Lae} \cdot C_{eq,Lae} + K_{eq,Lab} \cdot C_{eq,Lab} + K_{eq,\delta-\mathrm{Vin}} \cdot C_{eq,\delta-\mathrm{Vin}} + K_{eq,\varepsilon-\mathrm{Vin}} \cdot C_{eq,\varepsilon-\mathrm{Vin}}}} \quad \text{Eq (7)}$$

$$C_{eq,\varepsilon-\mathrm{Vin}} = \frac{C_{0,\varepsilon-\mathrm{Vin}} \cdot \left(\frac{V_S}{W}\right)}{\left(\frac{V_S}{W}\right) + \frac{K_{eq,\varepsilon-\mathrm{Vin}} \cdot qmax}{1+K_{eq,Res} \cdot C_{eq,Res} + K_{eq,Lae} \cdot C_{eq,Lae} + K_{eq,Lab} \cdot C_{eq,Lab} + K_{eq,\delta-\mathrm{Vin}} \cdot C_{eq,\delta-\mathrm{Vin}} + K_{eq,\varepsilon-\mathrm{Vin}} \cdot C_{eq,\varepsilon-\mathrm{Vin}}}} \quad \text{Eq (8)}$$

$$C_{eq,\delta-\mathrm{Vin}} = \frac{C_{0,\delta-\mathrm{Vin}} \cdot \left(\frac{V_S}{W}\right)}{\left(\frac{V_S}{W}\right) + \frac{K_{eq,\delta-\mathrm{Vin}} \cdot qmax}{1+K_{eq,Res} \cdot C_{eq,Res} + K_{eq,Lae} \cdot C_{eq,Lae} + K_{eq,Lab} \cdot C_{eq,Lab} + K_{eq,\delta-\mathrm{Vin}} \cdot C_{eq,\delta-\mathrm{Vin}} + K_{eq,\varepsilon-\mathrm{Vin}} \cdot C_{eq,\varepsilon-\mathrm{Vin}}}} \quad \text{Eq (9)}$$

$$C_{eq,Lae} = \frac{C_{0,Lae} \cdot \left(\frac{V_S}{W}\right)}{\left(\frac{V_S}{W}\right) + \frac{K_{eq,Lae} \cdot qmax}{1+K_{eq,Res} \cdot C_{eq,Res} + K_{eq,Lae} \cdot C_{eq,Lae} + K_{eq,Lab} \cdot C_{eq,Lab} + K_{eq,\delta-\mathrm{Vin}} \cdot C_{eq,\delta-\mathrm{Vin}} + K_{eq,\varepsilon-\mathrm{Vin}} \cdot C_{eq,\varepsilon-\mathrm{Vin}}}} \quad \text{Eq (10)}$$

Where $q_{eq,i}$ is the adsorbed quantity of stilbene i at equilibrium (mmol/g of dry resin); q_{max} is the resin adsorption capacity (mmol/g of dry resin) corresponding to the maximum quantity of stilbene that can be adsorbed onto the resin; $C_{0,i}$ and $C_{eq,i}$ are the concentrations of stilbene i initially and after adsorption at equilibrium (mmol/L) respectively; $K_{eq,i}$ is the equilibrium constant of stilbene i adsorption (L/mmol); V_S is the volume of culture medium (L); W is the resin dry weight (g); i refers to resveratrol, leachianol, labruscol, δ-viniferin, or ε-viniferin.

First, a tailor-made numerical method (Jacobi-like) was developed to solve the coupled nonlinear system of five equations, so as to estimate the theoretical composition of liquid and resin at equilibrium, for a given value of equilibrium constants $K_{eq,Res}$, $K_{eq,Lea}$, $K_{eq,Lab}$, $K_{eq,\delta-\mathrm{Vin}}$ and $K_{eq,\varepsilon-\mathrm{Vin}}$, and resin adsorption capacity q_{max}.

Then, it was combined to another tailor-made numerical method conceived to optimize equilibrium constants and resin adsorption capacity to make the Langmuir model fit experimental adsorption isotherm for each stilbene, according to the least squares method (Residual Sum of Squares "RSS"), considering relative deviations.

The adsorption isotherm experiments were conducted as follows: 0.5 g of dry resin were added in 125 mL shake flasks together with 20 mL of culture medium at different initial concentrations (the liquid was diluted by factors of 0.25, 0.5, 0.7, 1, or concentrated 1.5 and 2 times) and the flasks were agitated

overnight (140 rpm, 25 ºC). The adsorbed quantities of stilbene i at equilibrium, $\boldsymbol{q_{eq,i}}$, were calculated using Eq. (1) from measured value of $\boldsymbol{C_{0,i}}$ and $\boldsymbol{C_{eq,i}}$.

The confidence intervals of $K_{eq,i}$ and q_{max}were estimated by statistical analysis. They correspond to all sets of $K_{eq,i}$ and q_{max} values that lead to a RSS below a threshold, RSS_{max} for each stilbene adsorption isotherm. RSS_{max} corresponds to the maximum value of RSS that could be only explained by experimental uncertainty. It was estimated for each stilbene adsorption isotherm from the sum of squared standard deviation on each experimental point (according to the upper-tail one-sided critical value of the Chi-square distribution with significance level, α, equals to 0.05). The confidence interval of affinity coefficients $K_{aff,i}$, defined by Eq. (11), was also estimated because they are narrower than $K_{eq,i}$ confidence interval (estimation more accurate).

$$\boldsymbol{K_{aff,i} = K_{eq,i} \cdot q_{max}} \qquad \textbf{Eq (11)}$$

Finally, the model correlation and lack of fit, regarding the experimental data, was evaluated based on analysis of variance and classical Fisher's statistical tests.

2.7. Optimizations of the washing and desorption step

2.7.1. Optimization of the desorption solution ethanol percentage and volume

0.25 g of dry resin and 10 mL of culture medium were added in 125 mL shake flasks covered with parafilm and aluminum foil, and agitated overnight (140 rpm, 25 ºC) to reach equilibrium. Afterwards, the resins were filtered, washed with Milli-Q water and mixed with 50 mL of aqueous solutions of different ethanol percentages (0, 10, 30, 50, 70, 90, and 100% v/v) for 24 hours. The desorbed quantity of each stilbene was calculated using Equation Eq (3).

The methodology for studying the influence of the desorption solution ratio (compared to resin mass) was performed identically as above. However, instead of different ethanol concentrations, a desorption solution of 70% ethanol was used at different ratios (40:1, 80:1, 120:1, 160:1, 200:1 and 240:1, eluent volume:mass of dry resin).

2.7.2. Optimization of the water quantity and pH during the washing step before desorption step

The influences of the water quantity and pH during the washing step after adsorption step on the final stilbenes content were studied. 0.5 g of dry resin collected from the adsorption isotherms experiment (therefore already loaded with stilbenes) were introduced in 125 mL shake flasks, together with water at 120:1 or 180:1 ratio (water volume: mass of dry resin) and at pH = 2 or pH = 7. The flasks were shaken for 90 min. at 160 rpm and 25 ºC, and the washing step was repeated twice. Then, the resins

were collected by filtration and eluted overnight with 70% ethanol solution at a liquid/solid ratio of 180/1.

The weight percentage of stilbenes was measured as follows: aluminum trays were weighted empty and loaded with the desorption eluent rich in stilbene molecules. The trays were dried for 24 h at 105 ºC in an ED Binder drying oven and weighted again. The content was calculated using Equation Eq (12):

$$Purity\ (\%) = \frac{\sum_{i=1}^{n} C_{d,i} \cdot V_d}{m_{solids}} \cdot 100 \qquad \text{Eq (12)}$$

Where, $C_{d,i}$ is the concentration of stilbene i in the desorption eluent, V_d is the volume of the desorption eluent and m_{solids} represents the total solids mass after drying.

2.8. Identification and quantification of the five stilbene derivatives

The identification and quantification were performed using high-performance liquid chromatography (HPLC) with a Vanquish system (ThermoScientific, USA) equipped with a diode array detector FG. Compounds were separated on an Accucore C18 AQ column from Thermo Scientific (2.6 µm, 3 × 100 mm). Elution was carried out with a mobile phase consisting of pure water (solvent A), acetonitrile (solvent B), and 0.1% formic acid in water (solvent C), with the proportion of solvent C held constant at 30%. The gradient program was as follows: 0-3 minutes, 20% to 35% B; 3-4 minutes, 35% to 60% B; 4-5 minutes, 60% B; 5-5.5 minutes, 60% to 20% B; 5.5-6.5 minutes, 20% B. The flow rate was maintained at 0.8 mL/min. UV detection was conducted at 320 and 210 nm. The limit of detection and the limit of quantification were 0.26 and 0.85 µg/ml respectively. Chromeleon 7.3 Software was utilized for chromatogram processing.

2.9. Data analyses

All experiments were performed at least in duplicates and the data are presented as average together with standard deviation. A statistical test for analysis of significantly different means (Tukey method) was done at a significance level $p < 0.05$. The validation tools utilized for assessing the goodness of fit for adsorption kinetic models are the coefficient of determination (R^2), Chi-square test (χ^2) and root-mean-square deviation (RMSD). For adsorption isotherms, an analysis of variance (ANOVA) and Fisher's statistical tests were performed to evaluate the correlation and lack of fit of Langmuir equilibrium model.

3. Results and discussion

3.1. Resins screening

Five macroporous polymeric resins from the AmberLite™ series were chosen as they were previously studied for the adsorption of *E*-resveratrol and other (poly)phenolic compounds from model solutions, plant extracts or plant cell cultures media [19,27]. Figure 1 shows the quantity of each stilbene adsorbed

onto 5 different adsorbent resins (in mg/g_{resin} and mg/m^2_{resin}) then desorbed into 70% EtOH solution (in mg/g_{resin}), as well as the total stilbenes quantity adsorbed then desorbed (mg/g_{resin}) and the corresponding overall desorption yield. The highest polyphenol concentration quantified in the initial culture medium corresponds to *E*-resveratrol (279.62 mg/L), followed by leachianol (197.28 mg/L), labruscol (96.99 mg/L), δ- viniferin (58.39 mg/L) and ε-viniferin (37.91 mg/L) in decreasing order.

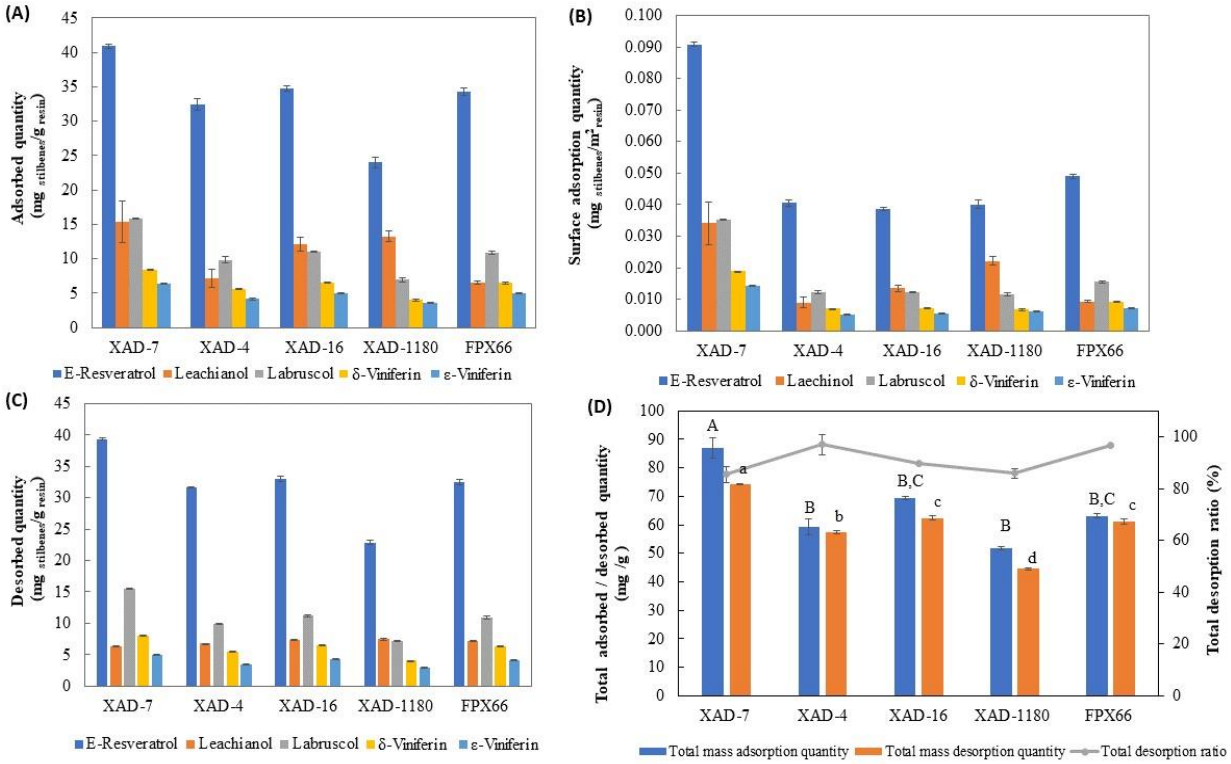

Figure 2. Adsorbed quantity (A) and surface adsorbed quantity (B) of Res, Lae, Lab, δ-Vin, ε-Vin onto XAD-7, XAD-4, XAD-16, XAD-1180 and FPX66 resins. Corresponding desorbed quantity into 70% EtOH solution (C) and total stilbenes quantity adsorbed then desorbed with the overall desorption yield (D). Columns having the same letter are not significantly different ($p < 0.05$).

A similar trend is observed regarding the adsorbed quantity of Res, Lab, δ-, and ε-Vin on all adsorbent resins (Figure 2, A). XAD-7 adsorbed the highest quantity (40.88 ± 0.40, 15.83 ± 0.15, 8.47 ± 0.02, and 6.40 ± 0.02 mg/g, respectively), followed by XAD-16 and FPX66 with comparable performances. Subsequently, XAD-4 shows lower adsorbed quantity, and XAD-1180 adsorbed the smallest quantity (24.04 ± 1.08, 6.96 ± 0.41, 3.99 ± 0.25, and 3.61 ± 0.11 mg/g, respectively). The adsorbed quantity on a polymeric resin depends on factors such as specific surface area, pore size, and hydrophobicity/hydrophilicity, affecting compound affinity. XAD-7, an acrylic ester polymer with moderate polarity (dipole moment: 1.8), absorbed the most stilbene derivatives. In contrast, other XAD resins and FPX66, derived from styrene and divinylbenzene monomers, exhibit strong non-polar characteristics. [28] hypothesized an adsorption mechanism of chlorogenic acid on XAD-7 and XAD-16: hydrogen bonds should occur between the hydroxyl groups of the polyphenolic compound and the

oxygen atoms of the acrylic ester polymer (XAD-7), while for XAD-16, non-covalent π-π stacking interactions would occur between the π electrons of the benzene rings of the styrene divinylbenzene (SDVB) adsorbent and adsorbate. These π-π interactions are known to occur between the π orbitals of aromatic rings and large aromatic molecules with multiple rings usually prefer a parallel arrangement [29]. Along the same idea, one could assume that the higher affinity of the targeted stilbene derivatives (Res, Lab, Lae, δ- and ε-Vin) on XAD-7 is due to the stronger and higher number of non-covalent hydrogen bonding interactions given by the several hydroxyl groups attached to the benzene rings of the polyphenols (Figure 1), compared to the weaker and maybe fewer π-π stacking interactions caused by the binding orientation of the molecules at the adsorbent surface, in the case of adsorption on SDVB resins (XAD-4, 16, 1180 and FPX 66). Moreover, hydrogen bonds are generally considered stronger than π-π stacking interactions as their energies are 1-40 kcal/mol and 2 kcal/mol, respectively [30].

In terms of surface adsorbed quantity ($mg_{stilbene}/m^2_{resin}$), XAD-7 is even more efficient (twice higher value) for all polyphenolic compounds (Figure 2, B) because of its smallest specific surface area (450 m^2/g). In comparison, XAD-16, which has a specific surface twice higher (900 m^2/g), adsorbed slightly less stilbene, so it corresponds to less than half of the surface adsorbed quantity on XAD-7. These results confirm the strong affinity of these stilbene derivatives on the slightly polar XAD-7.

As a consequence, XAD-7 displays the highest adsorption yields of *E*-resveratrol, leachianol, labruscol, δ- and ε-viniferins from the culture medium (73.46 ± 0.40%, 39.07 ± 10.81%, 82.01 ± 0.40%, 72.91 ± 0.15%, 84.86 ± 0.13%, respectively), while XAD-1180 shows the lowest adsorption yield (43.43 ± 2.43%, 33.90 ± 2.47%, 36.27 ± 2.54%, 34.56 ± 2.57%, 48.04 ± 2.01%, respectively). Besides, leachianol was the stilbene derivative with the smallest adsorption yield on all polymeric resins (Figure 3, A), which could be explained by its relatively low affinity for the adsorbent.

Finally, most stilbene derivatives show high desorption yield into 70% EtOH solution (> 95%) with all resins (Figure 3, B), except ε-viniferin (about 80% with all resins) and leachianol (40 to 60% with XAD-7, XAD-16 and XAD-1180). Nevertheless, overall desorption yield of stilbenes remained around 90% with all resins (Figure 2, D). Thus, XAD-7 was chosen to be used for all the further experiments, as the best compromise to adsorb then desorb into 70% EtOH the different stilbenes.

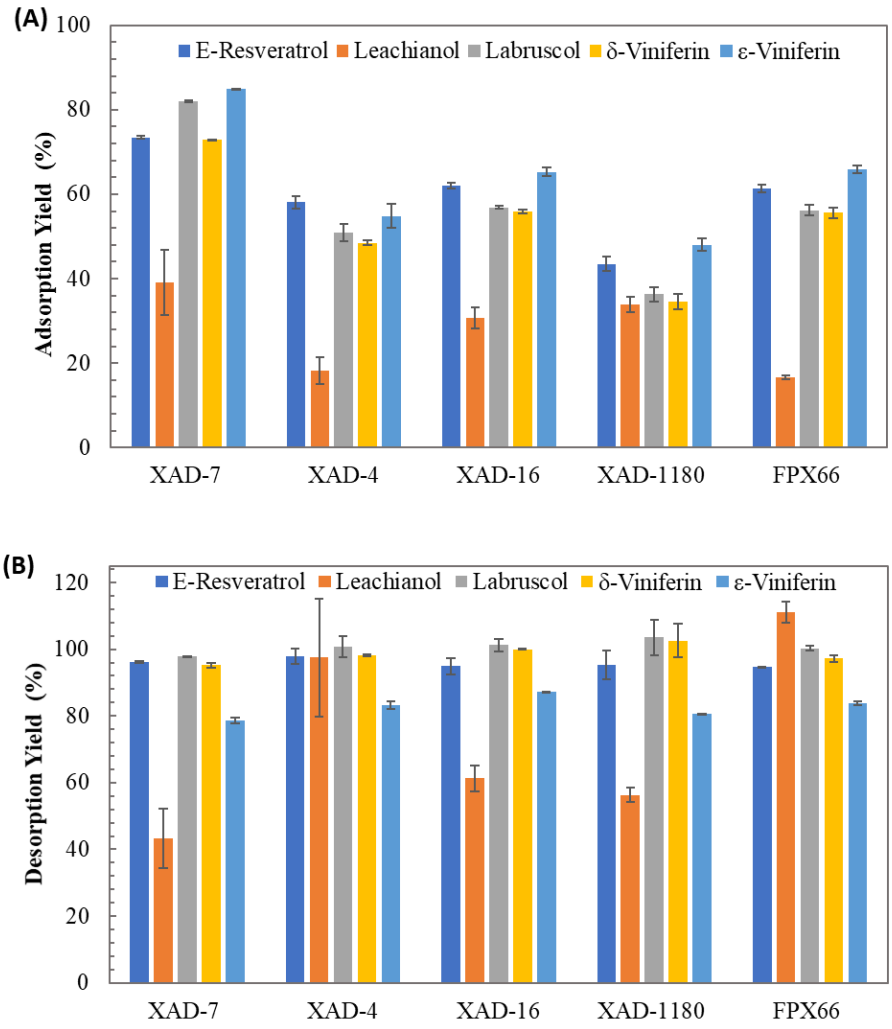

Figure 3. Overall adsorption (A) and desorption (B) yields of *E*-resveratrol, leachianol, labruscol, δ-viniferin, and ε-viniferin with XAD-7, XAD-4, XAD-16, XAD-1180 and FPX66 resins.

3.2. Adsorption and desorption kinetics

The adsorption and desorption kinetics of *E*-Res, Lae, Lab, δ-Vin, ε-Vin, and total stilbene compounds are shown in Figure 4. The adsorption kinetics of Res, Lab, δ- and ε-Vin (Figure 4, A) present a similar trend, where the adsorption takes place at a faster rate during the first 90 minutes (up to 89% of the q_{eq} is reached), followed by a period of slower adsorption until equilibrium is attained (240 to 360 min for Res and 180 min for Lab, δ- and ε-Vin). Despite the outlier point at 90 min (Figure 4, C), the adsorption process should be carried out for 240 min to achieve an equilibrium state of the overall system, regarding all data. In comparison, desorption takes place faster than adsorption, as the equilibrium is reached after approximately 60 minutes (Figures 4, B and D).

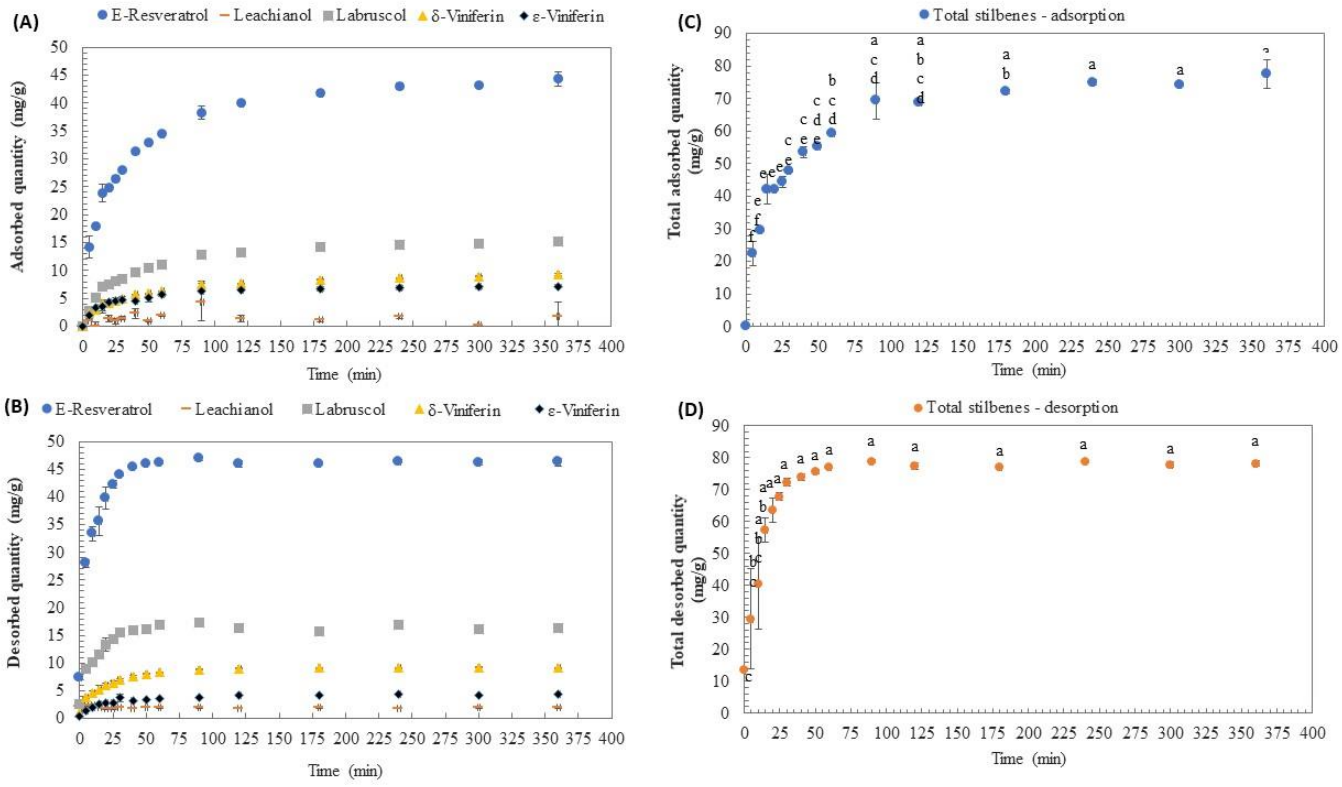

Figure 4. Adsorption and desorption kinetic curves of *E*-Res, Lea, Lab, δ- Vin, ε-Vin (A and B, respectively); adsorption and desorption curves of total stilbene derivatives (C and D, respectively) on XAD-7. Dots represent experimental data.

The experimental data was fitted with both linearized and non-linearized forms of the PSO and PFO models (Figure 5), which are widely used to describe the kinetics of adsorption [17]. Table 2 shows the kinetic parameters obtained for the adsorption of the individual stilbenes on XAD-7, together with the numerical validation methods used to assess the models correlation.

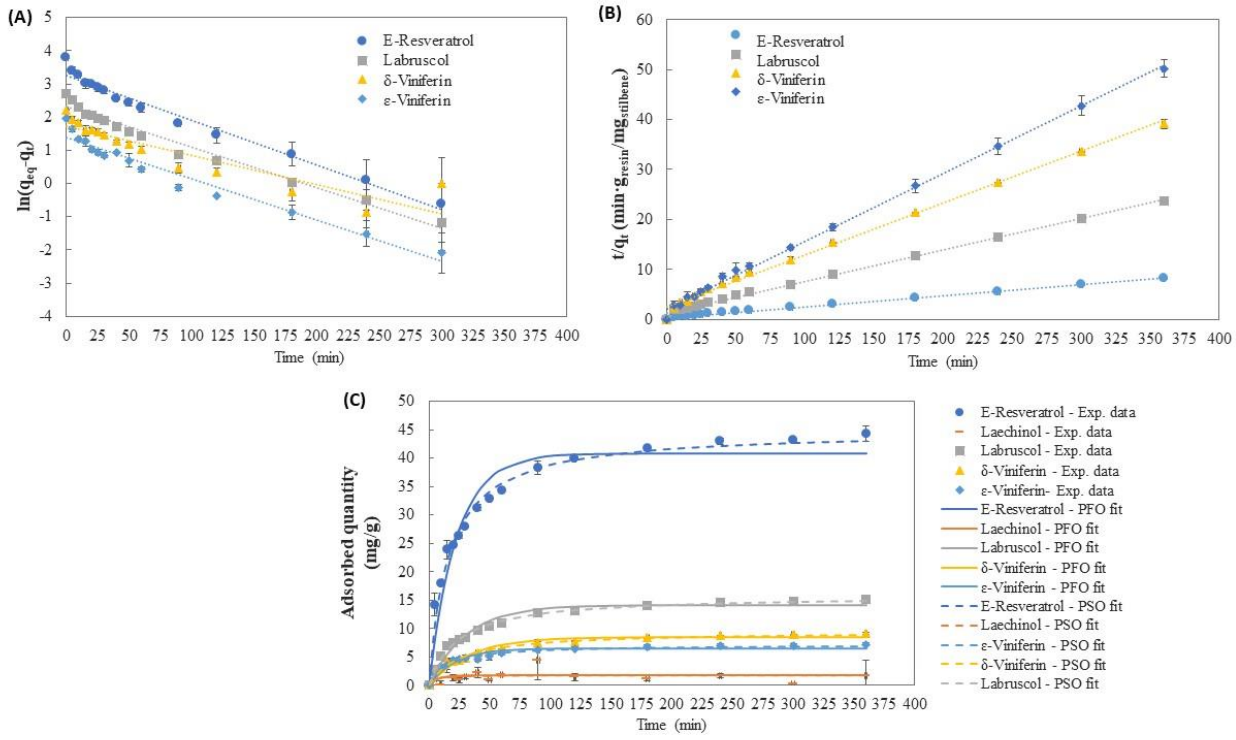

Figure 5. Linear fit of PFO model, linear fit of PSO model, and non-linear fit of PSO and PFO models (A, B, and C respectively).

Table 2. Kinetic parameters for the adsorption of Res, Lae, Lab, δ- and ε-Vin on XAD-7

Model	Rate constant, k	$q_{eq.calc}$ (mg/g)	% Error	R^2	χ2	RMSE
PFO Linear	k_1 (1/min)					
E-Resveratrol	0.014	25.88	-41.56	0.9686	-	-
Leachianol	NA	NA	NA	NA	-	-
Labruscol	0.012	10.03	-33.95	0.9714	-	-
δ-Viniferin	0.009	5.58	-39.42	0.8270	-	-
ε-Viniferin	0.012	4.02	-44.08	0.9556	-	-
PFO Non-linear						
E-Resveratrol	0.045	40.82	-7.84	-	0.295	8.04
Leachianol	0.141	1.72	-3.24	-	0.002	1.03
Labruscol	0.033	14.13	-6.99	-	0.080	0.64
δ-Viniferin	0.030	8.48	-7.89	-	0.062	0.35
ε-Viniferin	0.047	6.57	-8.47	-	0.056	0.27
PSO Linear	k_2 (g/(mg.min))					
E-Resveratrol	0.001	45.66	3.10	0.9982	-	-
Leachianol	0.673	1.38	-22.59	0.8825	-	-
Labruscol	0.003	15.90	4.67	0.9968	-	-
δ-Viniferin	0.004	9.62	4.52	0.9954	-	-
ε-Viniferin	0.009	7.39	2.90	0.9977	-	-
PSO Non-linear						
E-Resveratrol	0.001	44.99	1.58	-	0.011	1.62
Leachianol	0.185	1.78	-0.15	-	0.001	1.05
Labruscol	0.003	15.89	4.62	-	0.031	0.11
δ-Viniferin	0.004	9.55	3.73	-	0.012	0.11
ε-Viniferin	0.009	7.24	0.84	-	0.001	0.07
$q_{eq, exp}$ (mg/g):	Res = 44.29; Lae = 1.78; Lab = 15.19; δ-Vin = 9.21; ε-Vin = 7.18					

Looking at the linear regression of PFO and PSO models and the calculated adsorbed quantity at equilibrium q_{eq}, it can be observed that the PSO model fits better experimental data. For *E*-Res, Lab, δ- Vin and ε-Vin, the PSO model gives calculated q_{eq} values very close to experimental ones (only 2.9 to 4.7 % Error), compared to the PFO model (-34 to -44% Error). Moreover, the coefficients of determination (R^2) for the PSO linear regression were above 0.99, while for PFO less than 0.97. Therefore, as a first analysis, it could be assumed that the process followed a PSO kinetic model for adsorption on XAD-7. For leachianol, the linearized form of PFO could not be applied to the experimental data, and the PSO model resulted into a $R^2 = 0.8825$ and a quite different calculated adsorbed quantity at equilibrium (1.38 mg/g compared to 1.78 mg/g). Therefore, the adsorption kinetics of leachianol were not included in the graphical representations.

Application of the linearized forms of PSO and PFO implies transforming the kinetic data to a different scale (logarithmic scale), which comes with errors and biasness [31]. The linear form of the PFO model is disadvantaged because the equation becomes discontinuous when equilibrium is reached, and therefore the linear PSO model is greatly favored thanks to its mathematical form, even for systems which might actually fit the PFO kinetic model [31]. For these reasons, the non-linear forms of the two models were further used to fit the experimental data.

Analyzing the % of error, the non-linear PSO and PFO models fit better the experimental data compared to their linearized forms (Table 2), which is in line with other literature observations [32]. The % Error, χ^2, and RMSE resulted into small values for both non-linearized PSO and PFO models indicating a good fit to the experimental data. However, PSO model showed smaller differences between the calculated and experimental q_{eq} (-0.2 to 4.6 % Error) compared to PFO (-8.5 to -3.2 % Error) and smaller χ^2 and RMSE for all compounds. Therefore, one could say that the adsorption kinetics of Res, Lab, δ- and ε-Vin followed better a PSO model for adsorption on XAD-7. Revellame et al. [31] reported that 88.5% and 77.1% of the 350 surveyed scientific papers chose the PSO kinetic model as the suitable one to describe the adsorption process when linear and non-linear modeling, respectively, were employed. PSO was also the chosen model for the adsorption of polyphenols [33,34], chlorogenic acid [28] and resveratrol [35] on macroporous polymeric resins.

The transport mechanisms of solutes during the adsorption process are complex and studying the adsorption kinetics is relevant for determining the adsorption rate-limiting steps, which are generally film and intraparticle diffusion (IPD) processes [36]. The linearized form of the IPD model was used for the current work;

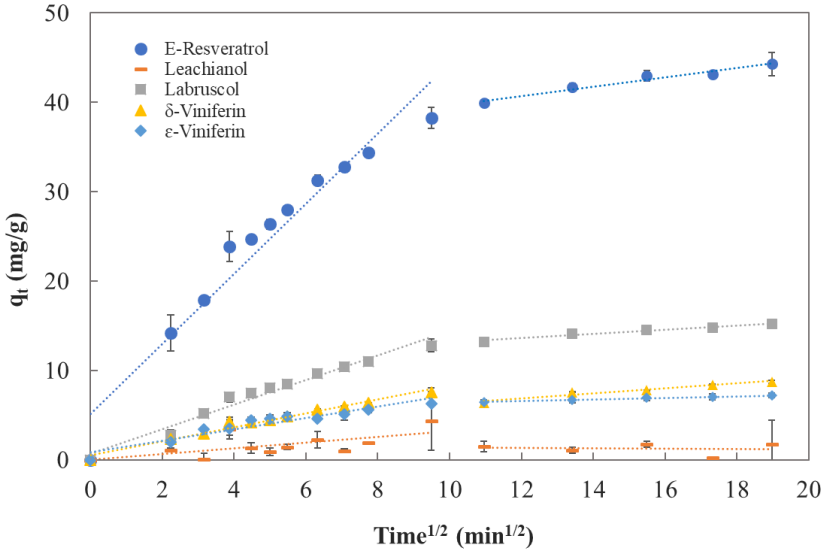

Figure 6 displays the linear regression of the diffusion curve and Table 3 the obtained parameters.

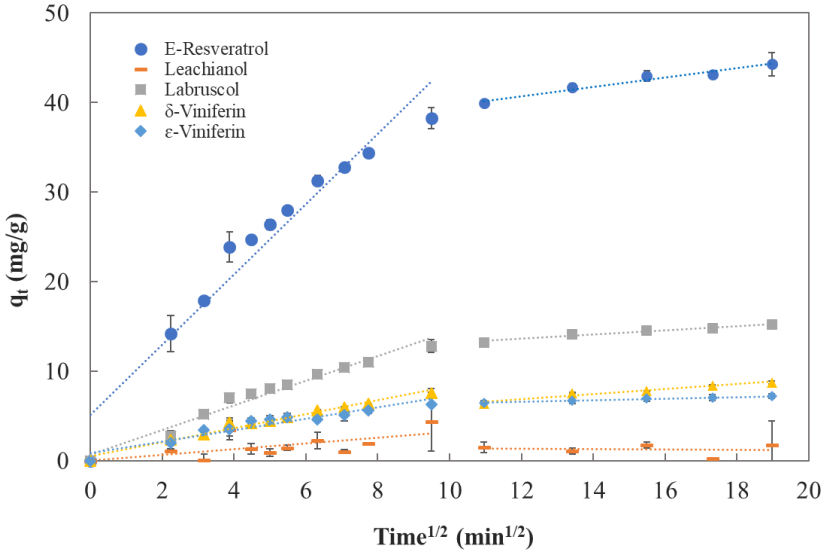

Figure 6. Linear fit of the intra-particle diffusion model.

Table 3. Kinetic parameters and regression coefficients of *E*-Res, Lae, Lab, δ-Vin and ε-Vin for the intra-particle diffusion model

Compound	**$k_{d,1}$ (mg/(g·min$^{1/2}$))**	**C_1 (mg/g)**	**R^2_1**	**$k_{d,2}$ (mg/(g·min$^{1/2}$))**	**C_2 (mg/g)**	**R^2_2**
E-Resveratrol	3.99	4.92	0.9499	0.52	34.53	0.9599
Leachianol	0.32	0.01	0.4252	0	1.54	0.0075

Labruscol	1.37	0.69	0.9686	0.24	10.77	0.9619
δ-Viniferin	0.78	0.56	0.9768	0.28	3.49	0.9534
ε-Viniferin	0.63	0.90	0.9128	0.08	5.61	0.9870

For all stilbene derivatives, an evolution in time with two different slopes can be observed, which could be associated to a two-step adsorption process. The first stage takes place faster, being characterized by higher adsorption rates $k_{d,1}$ (0.63-3.99 mg/(g·min$^{1/2}$)), and lower C_1 values (0.56-4.94 mg/g). This is followed by a slower adsorption step, wherein the rate constant decreased by 3 to 8 folds and C_2 increased up to 15 folds. R^2 values for *ε*-Res, Lab, δ-Vin, and ε-Vin range from 0.91 to 0.99. However, the IPD model poorly describes leachianol adsorption according to low determination coefficients (R^2_1 = 0.4252 and R^2_2 = 0.0075). The same step-wise evolution was observed by other scientists for the adsorption of chlorogenic acid on XAD-7 and XAD-16 [28], total phenolic compounds on HP20 [33], and flavonoids on XAD-16 and XAD-4 [37].

Previous explanations link the initial stage to diffusional transport through a boundary layer, followed by intra-particle diffusion. Elevated $k_{d,1}$ values indicate low diffusion resistance in the first stage, minimizing the boundary layer's impact. Slower $k_{d,2}$ (0.08-0.82 mg/(g·min$^{1/2}$)) signifies increased diffusion resistance in the second stage, limiting adsorption. This limitation is attributed to intra-particle diffusion, impeding about 10% of stilbenes. Stilbene derivative plots, not intersecting the origin, suggest additional transport mechanisms beyond IPD constrain the adsorption rate [33].

3.3. Adsorption isotherms

Figure displays the equilibrium between $q_{eq,i}$, the quantity of stilbenes adsorbed on the solid phase (mmol/g) and $C_{eq,i}$, the concentration of stilbenes in the aqueous liquid (mmol/L). The plot contains the points obtained experimentally and those resulting from the solving and optimization of the competitive Langmuir model by numerical methods.

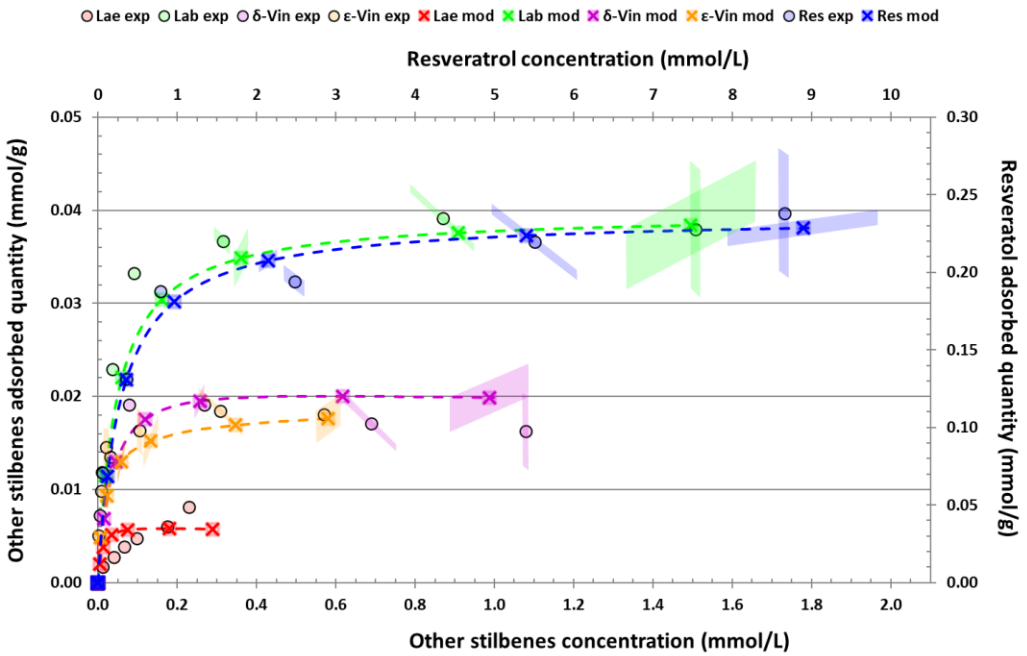

Figure 7. Experimental ("*Exp"*, circles) and modeled (*"Mod"*, X cross) adsorption isotherms of *E*-Res, Lae, Lab, ε-Vin, and δ-Vin when using XAD-7 resin. Standard deviations on concentration and adsorbed quantity are displayed as uncertainty areas around circles or X cross, for experimental and modeled points. The dashed curves represent modeled isotherm curves.

For all stilbenes, the adsorbed quantity ($q_{eq,i}$) exhibits a rapid increase at low concentrations, reaching a plateau at higher concentrations. The swift adsorption at the onset is attributed to the abundance of free adsorption sites, and the high affinity of stilbenes for XAD-7 resin. The plateau observed at high concentrations confirms a monolayer coverage on the adsorbent surface. Once fully saturated, further increases in stilbene concentration in the liquid phase do not result in additional adsorption onto the resin [38]. It is noteworthy that saturation was achieved from an initial concentration corresponding to the original culture medium, approximately 3.07 mg stilbenes/mL (10.5 mmol/L) with a solid-liquid ratio of 25 mg resin/mL.

To evaluate if the competitive Langmuir model is significantly correlated to the experimental data and fits them well (negligible lack of fit), an analysis of variance and Fisher's statistical tests were performed. Table 4 shows, for each stilbene, the coefficient of determination (R^2), F values for both correlation and lack of fit tests and their corresponding *p*-value (if the p-value is below 0.05, the corresponding F value tested is considered significant statistically).

Table 4. Statistical analysis of the competitive Langmuir model for adsorption isotherms with the XAD-7 resin

	R^2	$F_{correlation}$	*p*-value$_C$	$F_{lack\ of\ fit}$	*p*-value$_{LF}$
Resveratrol	0.996	1269	9.3 10-12	0.00	1.0

Leachianol	0.836	22.9	$2.9\ 10^{-4}$	16.2	$2.8\ 10^{-3}$
Labruscol	0.995	864	5.2 10-11	0.00	1.0
δ-Viniferin	0.984	271	$9.2\ 10^{-9}$	0.82	0.53
ε-Viniferin	0.985	296	$6.2\ 10^{-9}$	0.70	0.59

All compounds display very high R^2 values above 0.98, except leachianol but still high (0.836). It means that the competitive Langmuir model can explain most of the experimental data variance. However, to evaluate the quality of this model, the Fisher's statistical tests are more reliable. The correlation between the Langmuir model and experimental adsorption isotherms is significant for all stilbenes, according to high $F_{correlation}$ values, corresponding to p-values below 0.05. Meanwhile, the Langmuir model lack of fit is not significant for all stilbenes, except for leachianol, according to low $F_{lack\ of\ fit}$ values, corresponding to p-values above 0.05. To conclude, the competitive Langmuir model is very good at describing adsorption isotherms of all stilbenes on XAD-7 resin.

Table 5 shows the confidence interval of Langmuir model parameters which were optimized to fit the experimental adsorption isotherm of each stilbene. The adsorption capacity (q_{max}) of XAD-7 resin ranges from 0.28 to 0.36 mmol/g, which represents about 64 to 82 mg/g of resveratrol (if it was the only stilbene adsorbed). It is coherent with the adsorbed quantity of stilbene which reached 0.27 ± 0.02 mmol/g (or 80.0 ± 4.8 mg/g), close to saturation, when the original culture medium was used with a solid-liquid ratio of 25 mg resin/mL. This estimation of resin adsorption capacity is important for upscaling purpose.

Table 5. Confidence intervals of XAD-7 resin parameters estimated from Langmuir model: adsorption capacity (q_{max}), affinity coefficients ($K_{aff,i}$), equilibrium constants ($K_{eq,i}$) and their ratios for comparison purpose

Parameter	**Measure Unit**	**Confidence interval**	
q_{max}	mmol/g	0.280	0.360
$K_{eq,Res}$		1.3	9.0
$K_{eq,Lae}$		1.0	10.3
$K_{eq,Lab}$	L/mmol	1.5	9.5
$K_{eq,\delta\text{-}Vin}$		0.9	8.0
$K_{eq,\varepsilon\text{-}Vin}$		1.6	12.0
$K_{aff,Res}$		0.42	2.61
$K_{aff,Lea}$	L/g	0.33	2.98
$K_{aff,Lab}$		0.48	2.76

$K_{aff,\delta\text{-Vin}}$	-	0.31	2.32
$K_{aff,\varepsilon\text{-Vin}}$		0.58	3.47
$K_{eq,Lea}/K_{eq,Res}$		62%	157%
$K_{eq,Lab}/K_{eq,Res}$		78%	153%
$K_{eq,\delta\text{-Vin}}/K_{eq,Res}$		42%	95%
$K_{eq,\varepsilon\text{-Vin}}/K_{eq,Res}$		97%	190%
$K_{eq,Lab}/K_{eq,Lea}$		70%	161%
$K_{eq,\delta\text{-Vin}}/K_{eq,Lea}$		42%	104%
$K_{eq,\varepsilon\text{-Vin}}/K_{eq,Lea}$		95 %	203%
$K_{eq,\delta\text{-Vin}}/K_{eq,Lab}$		41%	92%
$K_{eq,\varepsilon\text{-Vin}}/K_{eq,Lab}$		95%	179%
$K_{eq,\varepsilon\text{-Vin}}/K_{eq,\delta\text{-Vin}}$		142%	321%

$K_{eq,i}$indicates how strong is the interaction between the stilbene i and the XAD-7 resin, in comparison with the liquid phase. All stilbenes show high $K_{eq,i}$ value (> 900 L/mol), so a stronger attraction to resin than to solvent. $K_{aff,i}$ is a combination of $K_{eq,i}$ and q_{max}, which considers the strength and the potential number of interactions on adsorption sites. Thus, it represents the global affinity of stilbenes for the resin, compared to the liquid phase. At low stilbene concentration, $K_{aff,i}$ corresponds also to the resin/liquid partition coefficient, which is the ratio between stilbene quantity adsorbed onto the resin (mmol/g) and stilbene concentration in the liquid phase (mmol/L) at equilibrium. All stilbenes show high $K_{aff,i}$ values (> 300 L/kg) when using XAD-7 resin to adsorb them from culture medium.

Due to the large $K_{eq,i}$ and $K_{aff,i}$ confidence intervals, whose estimation was affected by their strong intercorrelation and also correlation with q_{max} (when fitting Langmuir model to experimental data), they cannot be used directly to compare the affinity of different stilbenes. More experiments at various initial stilbene concentrations, with more analytical replicates, would be necessary to get smaller interval. Nevertheless, confidence intervals of equilibrium constants ratio between any stilbenes, given in Table 4, are much narrower, and enable to roughly compare their affinity. Firstly, the equilibrium constants of resveratrol, labruscol and leachianol are not statistically different. Then, the equilibrium constant of δ-viniferin is significantly lower than that of resveratrol (5 to 58% lower) and labruscol (8 to 59% lower). Lastly, ε-viniferin presents the highest equilibrium coefficient, but still limited statistically (the lowest ratio value compared to resveratrol is 97%). In summary, the affinity of stilbenes can be ranked as follows: ε-viniferin > (labruscol, *E*-resveratrol, leachianol) > δ-viniferin. These findings align with a study by Lambert et al. in 2019, which investigated the simultaneous adsorption of *E*-resveratrol, pallidol, ε-viniferin, and δ-viniferin from a *Vitis labrusca* cell culture medium on XAD-7 resin. The authors applied a Langmuir isotherm model with competition and reported their estimation of resin capacity and affinity constants (q_{max} ≈ 0.17 mmol/g, $K_{aff,Res}$ ≈ 7.3 L/g, $K_{aff,Pal}$ ≈ 5.5 L/g, and $K_{aff,\delta-\text{vin}}$ and $K_{aff,\epsilon-\text{vin}}$ ≈ 2.8 L/g) [13].

Viniferins, labruscol, and laechianol are not very common stilbenes, and therefore only resveratrol represents the compound which was previously studied in adsorption processes by multiple researchers. Xiong et al. [35] fitted the adsorption isotherms of resveratrol on ADS-5 macroporous resin from the extracts of peanut sprout with a single-solute Langmuir model and reported a q_{max} = 35.21 mg/g (0.154 mmol/g) and K_L = 1.514 L/mg (345.71 L/mmol). The results are not close to what was observed in the present study. However, the differences could be explained firstly by the use of a different adsorbent, which has a major influence on the affinity, and secondly by the use of different starting liquids (extract of peanut sprouts versus fermentation broth from grapevine cells). On the other hand, Silva et al. [39] studied the adsorption of a model aqueous solution of resveratrol on the XAD-7 resin. The maximum adsorption capacity obtained was q_{max} = 11 mg/g $_{wet\ resin}$ and K_L = 0.53 ± 0.03 L/mg (121 L/mmol). It can be hypothesized that the lower constant values in the current study are probably due to inhibitory effects given by the presence of other competing stilbene molecules and by the complex nature of the mixture (cell culture media containing vitamins, proteins, sugars, etc.), leading to lower adsorption affinities [26]. In contrast to the present work, Silva et al. carried out a study using a pure solution of resveratrol, and therefore no other molecules could inhibit its adsorption on XAD-7.

Finally, Lambert et al. [40] conducted a very similar study regarding the simultaneous adsorption of resveratrol, pallidol, ε-viniferin and δ-viniferin from a *Vitis labrusca* cell fermentation broth on the XAD-7 resin. The researchers applied a Langmuir isotherm model with competition and reported a $q_{max} \approx 0.168$ mmol/g, $K_{aff,Res}$ = 7 L/g, $K_{aff,Pallidol}$ = 5.5 L/g and $K_{aff,\ \varepsilon\text{- and }\delta\text{-Vin}}$ = 2.75 L/g. The affinity constants are the closest to the findings reported in the current study, and the dissimilarities could be explained by differences in the culture medium used and the experimental methodology.

3.4. Optimization of the washing and desorption steps

The impact of ethanol percentage in solution on stilbene desorption was studied to determine the optimal desorbent composition. From Figure8 (A) it can be observed that when only Milli-Q water or a very low percentage of ethanol solution were used, the desorbed quantity (q_d) was very low (1.11 ± 0.02 mg/g and 6.62 ± 0.26 mg/g, respectively). Then, the desorbed quantity increased while increasing the ethanol percentage until reaching a plateau around 60 mg/g from 70 to 100% (v/v) ethanol. Thus, using ethanol percentages higher than 70% (v/v) does not increase significantly the total amount of desorbed molecules ($p > 0.05$), while employing smaller content between 0 and 50% (v/v) decrease the desorbed quantity significantly ($p < 0.05$). Therefore, a desorption eluent containing 70% ethanol and 30% Milli-Q water (v/v) represents an optimum composition for the desorption of the 5 stilbenes molecules from XAD-7 resin beads.

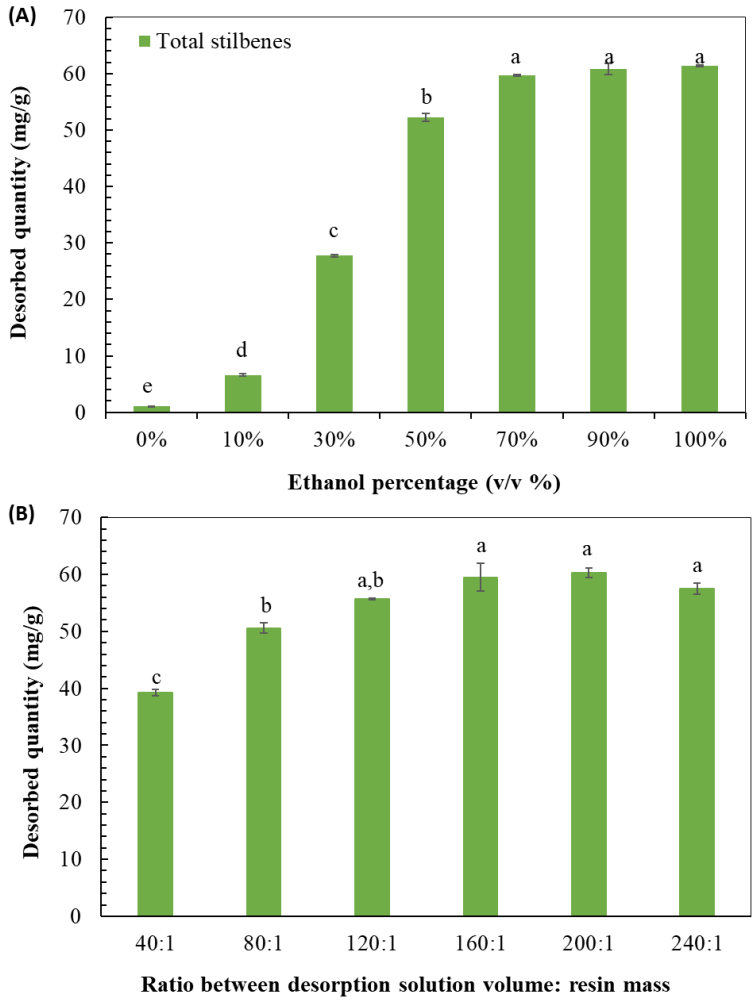

Figure 8. Influence of ethanol solution percentage **(A)** and of the ratio between desorption solution volume and resin mass **(B)** on the total desorbed quantity of stilbenes. Data are presented as an average of duplicates, and standard deviations as error bars. Different small letters indicate significant differences (ANOVA test, $p < 0.05$).

Furthermore, results show that the ratio between desorbent volume and resin mass impacts significantly the total desorbed quantity of stilbene (Figure8, B). The lowest q_d values were recorded for the smallest $V_{desorbent}$:m_{resin} ratios of 40:1 and 80:1 (39.26 ± 0.51 and 50.58 ± 0.94 mg/g, respectively), followed by increasingly higher desorbed quantity until a plateau around 60 mg/g from a ratio 160:1. Therefore, the most efficient ratio for both optimum desorption and solvent consumption is 160:1.

The desorption of stilbene from resin into ethanol solution is due to the competition between stilbene attraction by resin adsorption site and stilbene attraction into the solvent, which can be resumed by stilbene affinity difference for both phases. As for adsorption, stilbene distribution between both phases at equilibrium can be represented by desorption isotherms, which represents the remaining stilbene quantity on resin (mg/g) in function of final stilbene concentration in ethanol solution. According to the study of adsorption isotherms, the Langmuir model with competition well described stilbene adsorption

onto resin XAD-7. Therefore, it must be also good at describing stilbene desorption into ethanol by adjusting equilibrium constants ($K_{eq,i}$) but keeping the same resin adsorption capacity (q_{max}). In case of desorption into ethanol, $K_{eq,i}$ must be much lower because of better stilbene affinity for ethanol than for water, which lead to a relative lower affinity for resin. Consequently, it is expected to observe increase of desorbed stilbene quantity into desorbent solution when ethanol percentage increase, until reaching a plateau corresponding to the complete desorption of stilbene when the remaining stilbene quantity on resin is close to 0. Besides, desorption isotherms explain also the increase of desorbed stilbene quantity when increasing the ratio between desorbent volume and resin mass. Indeed, higher is the desorbent volume, lower is the stilbene concentration in solution so lower is the remaining stilbene quantity on resin, until reaching the same plateau corresponding to the complete desorption of stilbene when the remaining stilbene quantity on resin is close to 0 [41].

Different aspects of the water-washing step were studied for their potential impact on the final content of stilbenes, and subsequently on the process efficiency. Results are shown in Figure9.

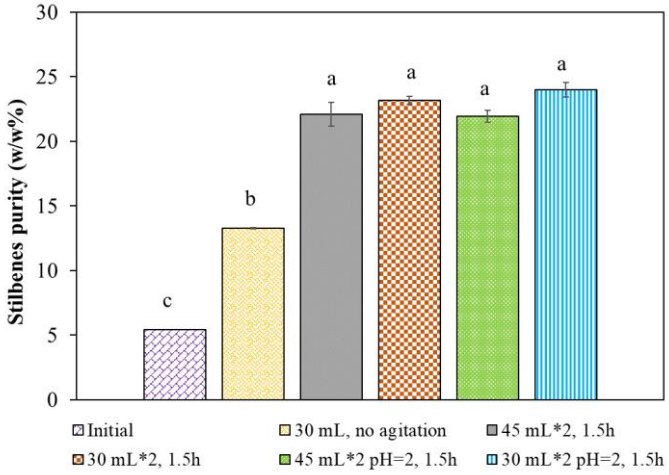

Figure 9. Influence of the water quantity, pH, and washing time on final stilbenes purity. Data are presented as an average of duplicates, and standard deviations as error bars. Different small letters indicate significant differences ($p < 0.05$)

Stilbenes purity can be increased from 5.41 w/w % to 13.29 ± 0.05 w/w % when only using XAD-7 adsorbent and a simple washing step with 30 mL of water and no agitation of the resin. Nevertheless, washing the beads twice with the same quantity of water and under agitation for 90 minutes improved significantly the purity to 23.19 ± 0.31 w/w%. Following this, a higher volume of water (from 30 mL to 45 mL) and acidification of the suspension from pH = 7 to 2 were studied, but no significant differences were recorded. Stilbenes are hydrophobic compounds and their loss in the wastewater can be considered negligible (loss percentage between 0.52 and 0.64 %). In conclusion, a thorough washing step of the resin beads in-between the desorption and adsorption steps can remove water soluble compounds present in the initial culture medium, such as sugars (saccharose, fructose, glucose, methyl-β-cyclodextrin), vitamins and salts [42], and therefore increase the final purity of the five target polyphenols by 4.6 times.

Furthermore, an NMR analysis was conducted on the purified extracts (Figure S7 in the supplementary material). This analysis revealed the presence of a few fatty chains and sugars, primarily β-methylcyclodextrin, which is present in high concentrations in the cell culture media.

3.5. Cycling stability of XAD-7

Figure 10 shows the variation of total stilbenes quantity (expressed as mg/g) during each of the five adsorption-desorption cycle, initially (after resin washing), adsorbed and unadsorbed (after adsorption), then desorbed and undesorbed (after desorption and before resin washing). It displays also the corresponding adsorption and desorption yields, and total stilbenes purity across cycles.

The adsorbed quantity varies slightly between cycles (± 10 mg/g) but stabilizes around 55 mg/g after 5 cycles (Figure 10.A). This fluctuation is almost attributed to the small variation of total stilbenes concentration in the cell culture media before each adsorption cycle. Otherwise, the initial quantity (remaining after resin washing between cycles) has also a minor impact on adsorbed quantity because it remaines quite low and stabilizes around 25 mg/g). Consequently, the adsorption yield remains almost constant around 74% throughout the cycles (Figure 10.B).

The desorbed quantity remains also almost constant around 50 mg/g when XAD-7 is reused (Figure 10.A). That is why, the desorption yield is slightly lower during cycles I and III (80% instead of 90%) because a little more stilbene was adsorbed right previously (Figure 10.B).

Despite these small differences, XAD-7 demonstrates good and stable adsorption and desorption capacities after five cycles of reuse. Additionally, the purity of stilbenes remains consistent (Figure 10.C), indicating that it is beneficial to reuse the adsorbent multiple times before disposal.

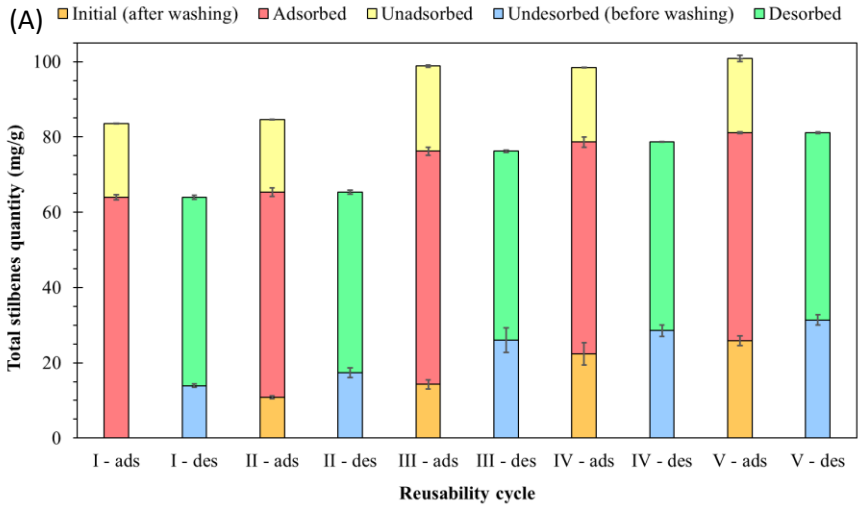

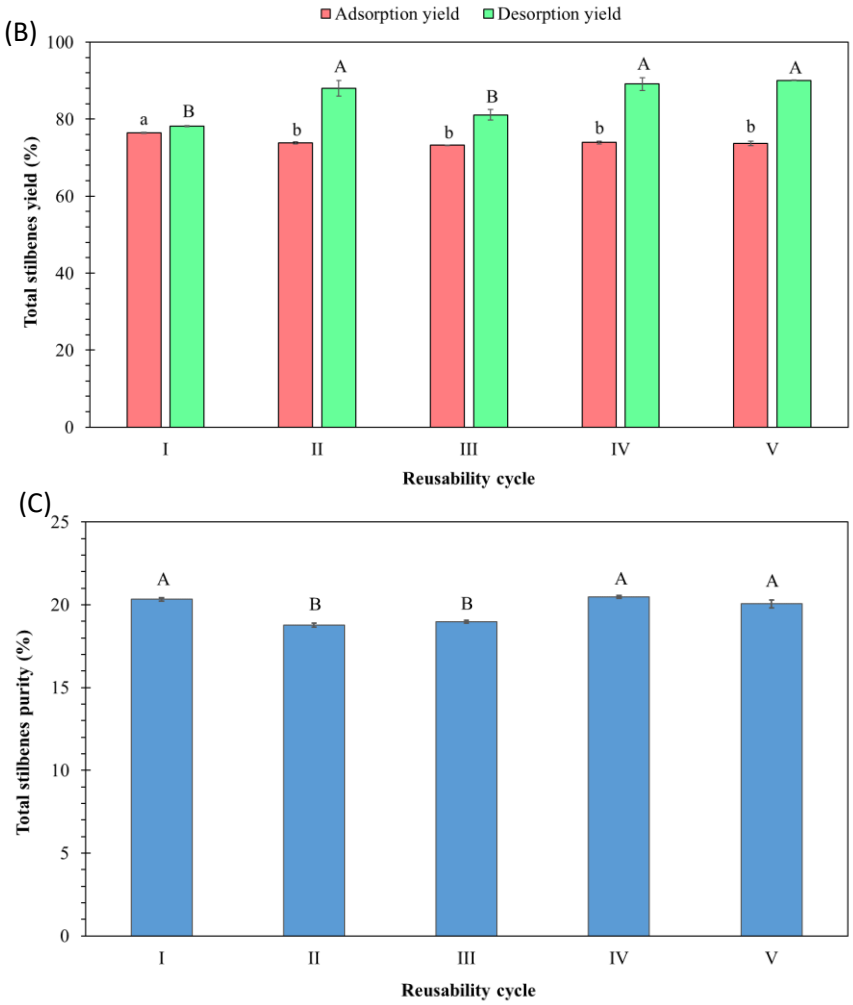

Figure 10. The variation of the total stilbenes quantity initially (after resin washing), adsorbed and unadsorbed (after adsorption), desorbed and undesorbed (after desorption and before resin washing) (A), of the corresponding adsorption and desorption yields (B) and of the total stilbenes purity after each of the five adsorption-desorption cycles (C). Columns having the same letter are not significantly different ($p<0.05$). Data are presented as average of duplicates ± standard deviations as error bars.

Conclusion

This study focused on the recovery and purification of *E*-resveratrol, labruscol, leachianol, ε-viniferin, and δ-viniferin from grapevine cell cultures medium by adsorption onto Amberlite macroporous resins. Among the five screened macroporous polymeric resins, XAD-7 exhibited the highest adsorption and desorption performance for total stilbenes in the first stage. The adsorption kinetics on XAD-7 followed a pseudo-second order model, with optimal adsorption achieved in 240 min and desorption in 60 minutes. Intraparticle diffusion within the adsorbent's pores limited the adsorption rate of approximately the last 10% of stilbenes. Moving to the third stage, the multicomponent Langmuir model with competition fitted well with experimental data, suggesting a mono-layer adsorption behavior. Stilbene

adsorption capacity of XAD-7 was estimated between 0.28 and 0.36 mmol/g_{resin}, which is consistent with the maximum adsorbed quantities observed previously (about 60 mg/g). Moreover, the relative affinity of different stilbenes towards the resin ranked as ε-viniferin > (labruscol, *E*-resveratrol, leachianol) > δ-viniferin.

The Langmuir equilibrium model provided time-saving advantages, enabling the accurate estimation of adsorbed quantity of each stilbene depending on operating conditions, knowing the resin adsorption capacity and equilibrium constants. Complete stilbene desorption was achieved using a 70% (v/v) ethanol aqueous solution at a 160:1 ratio (desorbent volume:resin mass). Overall, utilizing the slightly polar XAD-7 resin in batch operation, coupled with optimized water washing, increased stilbenes content by 4.6 times. The impurities in the final desorption solution were identified as mainly sugars (methyl-β-cyclodextrin).

The research indicates a highly encouraging prospect for employing XAD-7 as a food-grade and biocompatible adsorbent in the purification of stilbenes, showcasing their potential application in an in-situ product recovery approach from bioreactors. This innovative method holds promise for enhancing the efficiency and sustainability of stilbenes purification. The purified stilbenes obtained through this process could find diverse applications in sectors such as food, and pharmaceuticals, owing to their enhanced quality and purity.

Acknowledgement

The authors acknowledge the ANR for Glycostil project (grant ANR-20-CE43-0012) and the financial support of the communauté urbaine du Grand Reims, Département de la Marne, Région Grand Est and European Union (FEDER Grand Est 2021-2027) to the Chair of Biotechnology of CentraleSupélec, the URD Agro-Biotechnologies Industrielles and the Centre Européen de Biotechnologie et de Bioéconomie (CEBB).

References

[1] P. Pecyna, J. Wargula, M. Murias, M. Kucinska, More Than Resveratrol: New Insights into Stilbene-Based Compounds, Biomolecules 10 (2020) 1111. https://doi.org/10.3390/biom10081111.

[2] T. Teka, L. Zhang, X. Ge, Y. Li, L. Han, X. Yan, Stilbenes: Source plants, chemistry, biosynthesis, pharmacology, application and problems related to their clinical Application-A comprehensive review, Phytochemistry 197 (2022) 113128. https://doi.org/10.1016/j.phytochem.2022.113128.

[3] X. Su, D. Zhou, N. Li, Chapter 8 - Bioactive stilbenes from plants, in: Atta-ur-Rahman (Ed.), Studies in Natural Products Chemistry, Elsevier, 2022: pp. 265–403. https://doi.org/10.1016/B978-0-323-91097-2.00006-6.

[4] E. Multia, Potential and utilization of water extracts from spruce bark, 2018. https://doi.org/10.13140/RG.2.2.18886.16963/1.

[5] H. Kanda, K. Oishi, S. Machmudah, Wahyudiono, M. Goto, Ethanol-free extraction of resveratrol and its glycoside from Japanese knotweed rhizome by liquefied dimethyl ether without pretreatments, Asia-Pacific Journal of Chemical Engineering 16 (2021) e2600. https://doi.org/10.1002/apj.2600.
[6] G. Navarro, E. Martínez-Pinilla, R. Ortiz, V. Noé, C.J. Ciudad, R. Franco, Resveratrol and Related Stilbenoids, Nutraceutical/Dietary Complements with Health-Promoting Actions: Industrial Production, Safety, and the Search for Mode of Action, Compr Rev Food Sci Food Saf 17 (2018) 808–826. https://doi.org/10.1111/1541-4337.12359.
[7] I. Soural, N. Vrchotová, J. Tříska, J. Balík, Š. Horník, P. Cuřínová, J. Sýkora, Various extraction methods for obtaining stilbenes from grape cane of Vitis vinifera L, Molecules 20 (2015) 6093–6112. https://doi.org/10.3390/molecules20046093.
[8] M.-L. Tang, P. Peng, Z.-Y. Liu, J. Zhang, J.-M. Yu, X. Sun, Sulfoxide-Based Enantioselective Nazarov Cyclization: Divergent Syntheses of (+)-Isopaucifloral F, (+)-Quadrangularin A, and (+)-Pallidol, Chemistry – A European Journal 22 (2016) 14535–14539. https://doi.org/10.1002/chem.201603664.
[9] M. Sako, H. Hosokawa, T. Ito, M. Iinuma, Regioselective Oxidative Coupling of 4-Hydroxystilbenes: Synthesis of Resveratrol and ε-Viniferin (E)-Dehydrodimers, J. Org. Chem. 69 (2004) 2598–2600. https://doi.org/10.1021/jo035791c.
[10] C. Ponzoni, E. Beneventi, M.R. Cramarossa, S. Raimondi, G. Trevisi, U.M. Pagnoni, S. Riva, L. Forti, Laccase-Catalyzed Dimerization of Hydroxystilbenes, Advanced Synthesis & Catalysis 349 (2007) 1497–1506. https://doi.org/10.1002/adsc.200700043.
[11] R. Huber, A. Koval, L. Marcourt, M. Héritier, S. Schnee, E. Michellod, L. Scapozza, V.L. Katanaev, J.-L. Wolfender, K. Gindro, E. Ferreira Queiroz, Chemoenzymatic Synthesis of Original Stilbene Dimers Possessing Wnt Inhibition Activity in Triple-Negative Breast Cancer Cells Using the Enzymatic Secretome of Botrytis cinerea Pers., Front. Chem. 10 (2022). https://doi.org/10.3389/fchem.2022.881298.
[12] E. Sursin, A.L. Flourat, Z.L.E. Akissi, A. Martinez, N. Borie, C. Peyrot, E. Courot, J.-M. Nuzillard, J.-H. Renault, L. Voutquenne-Nazabadioko, F. Allais, Combining Laccase-Mediated Dimerization of Resveratrol and Centrifugal Partition Chromatography: Optimization of E-Labruscol Production and Identification of New Resveratrol Dimers, ACS Sustainable Chem. Eng. 11 (2023) 11559–11569. https://doi.org/10.1021/acssuschemeng.3c01997.
[13] C. Lambert, J. Lemaire, H. Auger, A. Guilleret, R. Reynaud, C. Clément, E. Courot, B. Taidi, Optimize, Modulate, and Scale-up Resveratrol and Resveratrol Dimers Bioproduction in Vitis labrusca L. Cell Suspension from Flasks to 20 L Bioreactor, Plants 8 (2019) 567. https://doi.org/10.3390/plants8120567.
[14] C. Aneklaphakij, P. Chamnanpuen, S. Bunsupa, V. Satitpatipan, Recent Green Technologies in Natural Stilbenoids Production and Extraction: The Next Chapter in the Cosmetic Industry, Cosmetics 9 (2022) 91. https://doi.org/10.3390/cosmetics9050091.
[15] N. Francezon, N.-S.-B.R. Meda, T. Stevanovic, Optimization of Bioactive Polyphenols Extraction from Picea Mariana Bark, Molecules 22 (2017) 2118. https://doi.org/10.3390/molecules22122118.
[16] R. Gutiérrez-Escobar, M.I. Fernández-Marín, T. Richard, A. Fernández-Morales, M. Carbú, C. Cebrian-Tarancón, M.J. Torija, B. Puertas, E. Cantos-Villar, Development and characterization of a pure stilbene extract from grapevine shoots for use as a preservative in wine, Food Control 121 (2021) 107684. https://doi.org/10.1016/j.foodcont.2020.107684.
[17] Z. Wei, Y. Zu, Y. Fu, W. Wang, C. Zhao, M. Luo, T. Efferth, Resin adsorption as a means to enrich rare stilbenes and coumarin from pigeon pea leaves extracts, Chemical Engineering Journal 172 (2011) 864–871. https://doi.org/10.1016/j.cej.2011.06.075.
[18] A. Abin-Bazaine, A.C. Trujillo, M. Olmos-Marquez, A. Abin-Bazaine, A.C. Trujillo, M. Olmos-Marquez, Adsorption Isotherms: Enlightenment of the Phenomenon of Adsorption, in: Wastewater Treatment, IntechOpen, 2022. https://doi.org/10.5772/intechopen.104260.
[19] A. Braga, M. Silva, J. Oliveira, A.R. Silva, P. Ferreira, M. Ottens, I. Rocha, N. Faria, An adsorptive bioprocess for production and recovery of resveratrol with Corynebacterium glutamicum, Journal of Chemical Technology & Biotechnology 93 (2018) 1661–1668. https://doi.org/10.1002/jctb.5538.

[20] M. Silva, L. Castellanos, M. Ottens, Capture and Purification of Polyphenols Using Functionalized Hydrophobic Resins, Ind. Eng. Chem. Res. 57 (2018) 5359–5369. https://doi.org/10.1021/acs.iecr.7b05071.
[21] Q. Xiong, Q. Zhang, D. Zhang, Y. Shi, C. Jiang, X. Shi, Preliminary separation and purification of resveratrol from extract of peanut (Arachis hypogaea) sprouts by macroporous adsorption resins, Food Chemistry 145 (2014) 1–7. https://doi.org/10.1016/j.foodchem.2013.07.140.
[22] T.T. Le, A. A, F. X, I. I, K. R, Adsorption of Phenolic Compounds from an Aqueous By-product of Sunflower Protein Extraction/Purification by Macroporous Resins, Journal of Chromatography & Separation Techniques 11 (2020) 1–12. https://doi.org/10.35248/2157-7064.20.11.435.
[23] S. Heravi, M. Rahimi, M. Shahriari, S. Nejad Ebrahimi, Enrichment of phenolic compounds from grape (*Vitis vinifera* L.) pomace extract using a macroporous resin and response surface methodology, Chemical Engineering Research and Design 183 (2022) 382–397. https://doi.org/10.1016/j.cherd.2022.05.011.
[24] D. Pradal, Eco-procédés d'extraction de polyphénols antioxydants à partir d'un co-produit agro-alimentaire, These de doctorat, Lille 1, 2016. https://theses.fr/2016LIL10190 (accessed July 10, 2024).
[25] D. Tungmunnithum, S. Drouet, A. Kabra, C. Hano, Enrichment in Antioxidant Flavonoids of Stamen Extracts from Nymphaea lotus L. Using Ultrasonic-Assisted Extraction and Macroporous Resin Adsorption, Antioxidants 9 (2020) 576. https://doi.org/10.3390/antiox9070576.
[26] C.R. Girish, Various isotherm models for multicomponent adsorption: A review, International Journal of Civil Engineering and Technology 8 (2017) 80–86.
[27] S.S. Mohammad, N. da Rocha Rodrigues, M.I.M.J. Barbosa, J.L.B. Junior, Useful separation and purification of anthocyanin compounds from grape skin pomace Alicante Bouschet using macroporous resins, J IRAN CHEM SOC 20 (2023) 875–883. https://doi.org/10.1007/s13738-022-02724-3.
[28] X. Framboisier, R. Kapel, I. Ioannou, A. Aymes, Adsorption of Phenolic Compounds from an Aqueous By-product of Sunflower Protein Extraction/Purification by Macroporous Resins, Journal of Chromatography & Separation Techniques (2020).
[29] R. Thakuria, N.K. Nath, B.K. Saha, The Nature and Applications of π–π Interactions: A Perspective, Crystal Growth & Design 19 (2019) 523–528. https://doi.org/10.1021/acs.cgd.8b01630.
[30] T. Chen, M. Li, J. Liu, π–π Stacking Interaction: A Nondestructive and Facile Means in Material Engineering for Bioapplications, Crystal Growth & Design 18 (2018) 2765–2783. https://doi.org/10.1021/acs.cgd.7b01503.
[31] E.D. Revellame, D.L. Fortela, W. Sharp, R. Hernandez, M.E. Zappi, Adsorption kinetic modeling using pseudo-first order and pseudo-second order rate laws: A review, Cleaner Engineering and Technology 1 (2020) 100032. https://doi.org/10.1016/j.clet.2020.100032.
[32] S. Zafar, N. Khalid, M. Daud, M. Mirza, Kinetic Studies of the Adsorption of Thorium Ions onto Rice Husk from Aqueous Media: Linear and Nonlinear Approach, 52 (2015) 14–19.
[33] L. Firdaous, B. Fertin, O. Khelissa, M. Dhainaut, N. Nedjar, G. Chataigné, L. Ouhoud, F. Lutin, P. Dhulster, Adsorptive removal of polyphenols from an alfalfa white proteins concentrate: Adsorbent screening, adsorption kinetics and equilibrium study, Separation and Purification Technology 178 (2017) 29–39. https://doi.org/10.1016/j.seppur.2017.01.009.
[34] S. Heravi, M. Rahimi, M. Shahriari, S. Nejad Ebrahimi, Enrichment of phenolic compounds from grape (Vitis vinifera L.) pomace extract using a macroporous resin and response surface methodology, Chemical Engineering Research and Design 183 (2022) 382–397. https://doi.org/10.1016/j.cherd.2022.05.011.
[35] Q. Xiong, Q. Zhang, D. Zhang, Y. Shi, C. Jiang, X. Shi, Preliminary separation and purification of resveratrol from extract of peanut (Arachis hypogaea) sprouts by macroporous adsorption resins, Food Chemistry 145 (2014) 1–7. https://doi.org/10.1016/j.foodchem.2013.07.140.
[36] E. Worch, Adsorption Technology in Water Treatment: Fundamentals, Processes, and Modeling, De Gruyter, 2012. https://doi.org/10.1515/9783110240238.
[37] Y. Dong, M. Zhao, D. Sun-Waterhouse, M. Zhuang, H. Chen, M. Feng, L. Lin, Absorption and desorption behaviour of the flavonoids from Glycyrrhiza glabra L. leaf on macroporous adsorption resins, Food Chemistry 168 (2015) 538–545. https://doi.org/10.1016/j.foodchem.2014.07.109.

[38] A. Abin-Bazaine, A.C. Trujillo, M. Olmos-Marquez, A. Abin-Bazaine, A.C. Trujillo, M. Olmos-Marquez, Adsorption Isotherms: Enlightenment of the Phenomenon of Adsorption, IntechOpen, 2022. https://doi.org/10.5772/intechopen.104260.
[39] O. 1. Modulate, and Scale-up Resveratrol and Resveratrol Dimers Bioproduction in Vitis labrusca L. Cell Suspension from Flasks to 20 L. Bioreactor, M. Silva, L. Castellanos, M. Ottens, Capture and Purification of Polyphenols Using Functionalized Hydrophobic Resins, Ind. Eng. Chem. Res. 57 (2018) 5359–5369. https://doi.org/10.1021/acs.iecr.7b05071.
[40] C. Lambert, J. Lemaire, H. Auger, A. Guilleret, R. Reynaud, C. Clément, E. Courot, B. Taidi, Optimize, Modulate, and Scale-up Resveratrol and Resveratrol Dimers Bioproduction in Vitis labrusca L. Cell Suspension from Flasks to 20 L Bioreactor, Plants 8 (2019) 567. https://doi.org/10.3390/plants8120567.
[41] T. Wang, S. Lu, Q. Xia, Z. Fang, S. Johnson, Separation and purification of amygdalin from thinned bayberry kernels by macroporous adsorption resins, Journal of Chromatography B 975 (2015) 52–58. https://doi.org/10.1016/j.jchromb.2014.10.038.
[42] G.J. Tortora, B.R. Funke, C.L. Case, Microbiology: An Introduction, Pearson, 2019.